Hindawi
Journal of Advanced Transportation
Volume 2022, Article ID 3073393, 17 pages
https://doi.org/10.1155/2022/3073393

Research Article

The Longitudinal Driving Behavior of a Vehicle Assisted with Lv2 Driving Automation: An Empirical Study

Rita Rodrigues[1,2] **Ana Bastos Silva**[1,2] **Luís Vasconcelos**[3,4] **and Álvaro Seco**[1,2]

[1]*Faculty of Science and Technology of the University of Coimbra, Coimbra, Portugal*
[2]*Rua Luís Reis Santos, Coimbra 3030-788, Portugal*
[3]*Polytechnic Institute of Viseu, Viseu, Portugal*
[4]*Campus Politécnico de Repeses, Viseu 3504-510, Portugal*

Correspondence should be addressed to Rita Rodrigues; 89ritarodrigues@gmail.com

Received 22 March 2022; Revised 15 July 2022; Accepted 19 September 2022; Published 23 November 2022

Academic Editor: Haneen Farah

As the number of automated vehicles in our transportation system increases, it becomes increasingly important to understand how automation affects their driving behavior. This study defines and tests a methodology based on optimization methods to incorporate the longitudinal driving behavior of automated vehicles in the Wiedemann 99 car-following model. A pilot study was recently conducted in Portugal using a Mercedes-Benz of 2017 assisted with level 2 driving automation to gather empirical data. In total, 61 car-following events were used to support the calibration and validation tasks. The calibration error sustains the methodology's descriptive capability to simulate the driving behavior of AVs, and the validation error sustains that the calibrated model parameters can reproduce the dynamic driving behavior of AVs with reasonable consistency and robustness. A total of seven model parameters were estimated and are in line with the trends often described in the literature on automated vehicles but also highlight differences that can be explained by different development and deployment strategies. Nevertheless, since empirical data from automated vehicles are hard to get, the presented work findings are also valuable for improving and validating future modeling efforts.

1. Introduction

Technological advancements are changing the act of driving and revolutionizing our transportation system [1]. In particular, Automated Vehicles (AVs), which are motor vehicles equipped with driving automation technologies such as "hardware and software that are collectively capable of performing part or all of the dynamic driving tasks (DDT) on a sustained basis" [2], will make driving easier and eventually offer greater mobility to a wider range of people than ever before. They are also expected to enhance road safety, reduce emissions, and ease congestion. As a result, research regarding AVs has attracted considerable attention in recent years.

The extent to which technology can replace a human driver varies [2]. Therefore, driving automation is classified by the Society of Automotive Engineers (SAE) into six levels, ranging from no automation (level 0) to full automation (level 5), hereon as Lv0 to Lv5. In general, AVs use a combination of technologies (i.e., sensors, cameras, radar, and software) in order to perceive the world around the vehicle and then either provide information to the driver or take action when necessary. In this sense, advanced driver assistance systems (ADASs) are passive and active safety technologies designed to remove the human error component when operating any vehicle and form the basis of current and future driving automation technology.

Today, the most advanced vehicles available on the market operate at Lv2—partial driving automation. According to SAE taxonomy, these can provide sustained lateral and longitudinal control of the vehicle motion though limited to specific operational design domains (ODDs) (it refers to "operating conditions under which a given driving automation system or feature thereof is specifically designed to function, including, but not limited to, environmental, geographical, and time-of-day restrictions, and/or the requisite presence or absence of certain traffic or roadway characteristics" [2]). In other words, these can at times brake automatically, accelerate, and, unlike Lv1 systems, take over steering under certain circumstances. Even so, it is worth mentioning that features from Lv2 AVs can vary in terms of sophistication. Common features that fall under this category include following another vehicle while maintaining a predetermined distance, keeping the car centered within its lane by observing road markers, and stopping and restarting during traffic jams without driver intervention. More sophisticated Lv2 features can also change lanes after confirmation from the driver, who is responsible for properly using the turn signal. Despite the fact that Lv2 driving automation can handle these basic driving tasks, the driver must remain alert and ready to take control of the driving task, with or without warning. Mercedes-Benz Drive Pilot and similar systems from Tesla, Volvo, and Nissan are examples of partial automation.

While acknowledging the achievements in driving automation development for the past decades, there are still profound challenges and concerns in designing higher levels of automation, mainly centered around technology acceptance [3], human factors [4], technical [5], and legal concerns [6]. Hence, as the number of AVs with Lv2 systems is already increasing in our transportation networks, understanding how their driving behavior is affected by automation is fundamental to properly address challenges that may arise in the decades to come.

This study aims to define and test a methodology to incorporate the driving behavior of automated vehicles in the Wiedemann 99 car-following model, whose results can be applied to future modeling efforts. For this purpose, a pilot study was conducted in Portugal to gather empirical data representative of the longitudinal driving behavior of Lv2 AVs in real-world traffic. A total of 61 car-following events were collected and analyzed to support the calibration and validation procedures of the Wiedemann 99 car-following model. In the remainder of this paper, Section 2 presents the Wiedemann 99 model and reviews the existing literature. In Section 3, we discuss the methodology for data collection and car-following event extraction. Section 4 presents the calibration and validation procedures used, followed by Section 5 which reports the parameters estimates from the Wiedemann 99 model. At last, in Section 6, we conclude the paper with a critical discussion of our results.

2. Literature Review

Literature on car-following theory is vast. Over the past decades, different car-following models have emerged to replicate how a vehicle follows another in a given roadway. Researchers have explained these different approaches based on various driving strategies, commonly classified into stimulus-based, safety distance, desired measures, optimal velocity, and psychophysical models. Reviewing car-following models literature and introducing the different theories is beyond the scope of this study. Interested readers should see Aghabayk et al. [7] and Ahmed et al. [8] for a detailed review.

The car-following model is an important component of microscopic traffic simulation tools to describe the longitudinal driving behavior of vehicles. Among a number of commercially available microscopic simulation packages, Vissim and Aimsun are arguably two of the most known and widely used tools by scholars and practitioners [8, 9]. Basically, Vissim reproduces the longitudinal driving behavior of vehicles using the Wiedemann car-following model, while Aimsun uses the Gipps car-following model. Both are classic models developed from different angles to mimic the dynamic driving behavior of human-driven cars and thus have problems such as limited applicability when mimicking automated vehicles. For instance, the absence of a minimum safe car-following distance [10], vehicles reaching the equilibrium speed monotonically [11], and frequent oscillations of acceleration/deceleration [12] are some of the problems that make the traditional Gipps car-following model have the inability to describe different forms of driving automation (e.g., ACC) [13] and overall a quite poor performance when applied to AVs framework. On the other hand, the Wiedemann car-following model decides how the following vehicle behaves based on the reaction and perception abilities of the human driver, which makes this model also not the most suitable option to replicate the dynamics of automated driving systems [14]. Despite the shortcomings of both car-following models, the use of Vissim for modeling and analyzing a wide range of transportation network problems, particularly in the presence of AVs, has substantially grown in the last few years compared to other commercially available microscopic tools in the market [9, 15–17]. Hence, its car-following model is the subject of this research. Vissim has two different implementations of the car-following model: Wiedemann 74 and Wiedemann 99 [17]. In this regard, the Wiedemann 99 car-following model is more suitable than the 74 version for modeling the longitudinal driving behavior of AVs [17], which is the aim of this study.

Therefore, this Section begins with a comprehensive description of a version of the Wiedemann 99 car-following model that includes modifications introduced by the authors to simulate automated driving. Subsequently, we present a systematic literature review that compares model parameters often used to simulate the following behavior of AVs, such as those with Lv1 and Lv2 driving automation. We focus our attention on these levels since they represent the most popular types of vehicle automation that are presently in use in our public roadways. Lastly, we also review the methods used to estimate the model parameters discussed.

2.1. Wiedemann 99 Car-Following Model. In this study, the Wiedemann 99 car-following model introduced in Zhu et al. [18] is used. The equations that form the model were modified to remove the stochastic behavior of human drivers since automated driving is likely predictable and with deterministic behavior [8]. Wiedemann 99 (hereon also referred to as W99) belongs to a family of models known as

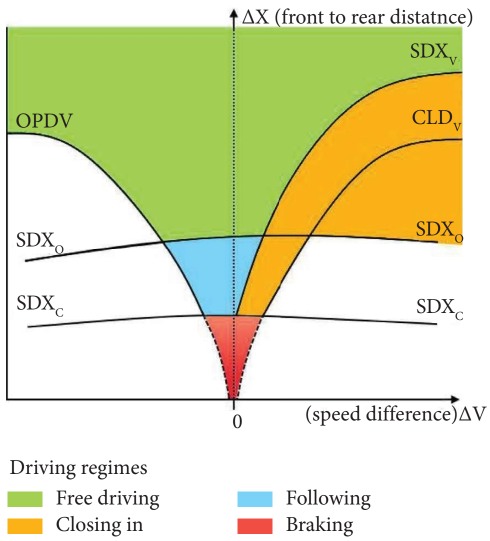

Figure 1: Wiedemann 99 car-following model driving regimes and thresholds adapted from PTV Vissim [17].

psychophysical car-following behaviors. The main idea behind it is that based on the distance (Δx) and speed (Δv) difference to the lead vehicle, the following vehicle is on one of four driving regimes: Free driving, Closing in, Following, and Emergency Braking, as shown in Figure 1.

A brief description of the driving regimes in the Wiedemann 99 car-following model is presented below:

Free Driving. The following vehicle will move at the desired speed uninfluenced by nearby vehicles.

Closing In. The following vehicle perceives at long distances a slower leader vehicle. During the closing process, the follower will start to reduce speed.

Following. In this regime, the follower vehicle will accelerate or decelerate to maintain a safe distance, relatively constant, based on the followers' perception of the leader vehicle speed at short distances.

Emergency Braking. The following vehicle will brake abruptly to avoid a collision and accelerate to come to the stationary stage.

Essentially, the driving behavior of a particular vehicle is considered in a car-following situation when it is under the influence of a leader. This situation will continue until the follower vehicle overtakes or until the leader starts to continuously increase speed [19].

The bounds of each driving regime are defined using various thresholds to determine changes in the behavior of the following vehicle, as shown in Figure 1. The physical meanings of these thresholds are as follows [17]:

SDX_c: minimum safe following distance (m).

SDX_0: maximum following distance (m).

SDX_v: distance threshold of speed difference at long distances (m).

SDV: perception threshold of speed difference at long distances (m/s).

$CLDV$: perception threshold of speed difference at short, decreasing distances (m/s).

$OPDV$: perception threshold of speed difference at short but increasing distances (m/s).

The output of the Wiedemann 99 model is the follower's acceleration or deceleration at time step $t+1$ based on the driving regime and stimulus coming from the leader vehicle at step t. Figure 2 presents an overview of the process of calculation.

More specifically, the acceleration of the following vehicle (denoted as a_n) at time step $t+1$ is computed based on governing equations used to predict the thresholds, relative speed (Δv), and relative position (Δx: front edge to rear-end distance) at time step t. We present below these equations (1)–(9), together with a brief explanation of all parameters according to the W99 car-following model in Figure 2.

$$\Delta v(t) = v_{n-1}(t) - v_n(t), \tag{1}$$

$$\Delta x(t) = x_{n-1}(t) - x_n(t) - L_{n-1}, \tag{2}$$

$$SDX_c = CC0 + CC1 \times V_{slower}, \tag{3}$$

$$V_{slower} = \begin{cases} v_n(t), & \text{if } \Delta v(t) > 0 \text{ or } LV_{acc}(t) < -1, \\ v_{n-1}(t), & \text{otherwise}, \end{cases} \tag{4}$$

$$SDX_0 = SDX_c + CC2, \tag{5}$$

$$SDX_v = SDX_0 + CC3 \times (\Delta v(t) - CC4), \tag{6}$$

$$SDV = CC6 \times (\Delta x(t) - L_{n-1})^2, \tag{7}$$

$$CLDV = \begin{cases} CC4 - SDV, & \text{if } \mathrm{v}_{n-1}(\mathrm{t}) > 0, \\ 0, & \text{otherwise}, \end{cases} \tag{8}$$

$$OPDV = \begin{cases} CC5 + SDV, & \text{if } \mathrm{v}_n(\mathrm{t}) > CC5, \\ SDV, & \text{otherwise}, \end{cases} \tag{9}$$

where the speed (m/s), position (m), and length (m) of the following vehicle are represented as v_n, x_n, and L_n, respectively. Similarly, the speed, position, and length of the leader vehicle are denoted as v_{n-1}, x_{n-1}, and L_{n-1}, respectively. LV_{acc} is the acceleration of the leader given in m/s^2, while VDES and a_{MAX} are used to describe the desired speed (m/s) and maximum acceleration (m/s^2) of the following vehicle, respectively. ΔT is the interval of time required for the subject vehicle to react to a changing situation, t is the time instant in seconds, and $CC0$ to $CC9$ are model parameters, that is, parameters that are adjustable in the model calibration process. Briefly, $CC0$ is the standstill gap (m), $CC1$ represents the headway time (s), $CC2$ describes the following variation (m), $CC3$ defines the threshold for entering the "following regime" (s), and $CC4$ and $CC5$ are the negative and positive "following" thresholds (m/s), respectively, while $CC6$ denotes the speed dependency of oscillation ($10^{-4} rad/s$), $CC7$ is the oscillation acceleration (m/s^2), $CC8$ designates the

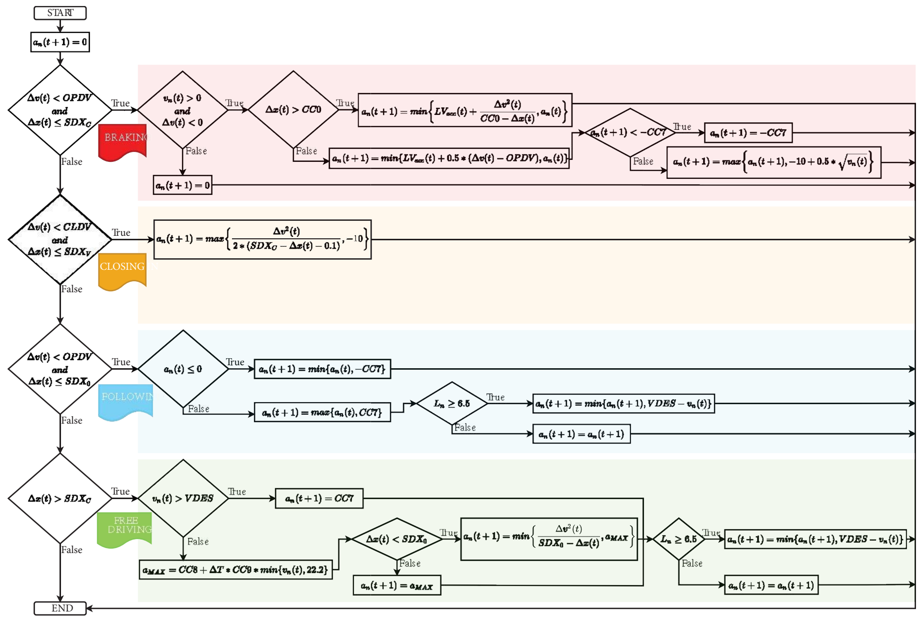

Figure 2: Process of calculation regarding the follower's acceleration in the W99 model modified from Zhu et al. [18].

standstill acceleration (m/s^2), and at last $CC9$ specifies the following vehicle acceleration at 80 km/h (m/s^2).

2.2. Model Parameters for AVs. Model parameters, such as those in the Wiedemann 99 car-following model, can be adjusted to reflect the longitudinal movement of the following vehicle as a function of its leader. These parameters have been widely investigated in a variety of studies concerning manually driven vehicles [18, 20–22]. However, there is also a growing body of evidence focusing on adjusting these model parameters in order to replicate the driving behavior of different AVs [8, 16, 23, 24]. In this context, the bulk of literature currently revolves around vehicles equipped with Lv1 systems, more specifically, with adaptive cruise control (ACC). This is understandable, given that this technology has existed for decades and serves as the foundation for future automobile intelligence [14]. It is worth mentioning that this literature also attempts to reproduce the driving behavior of AVs with cooperative adaptive cruise control (CACC) systems [25, 26]. The CACC is an extension of the ACC concept that enables vehicle-to-vehicle communication and is also classified as Lv1 driving automation. Although cooperative systems are still in the early stages of development, they have been included in our literature review to enrich the existing discussion.

Below, we present per parameter the relevant literature that attempts to simulate the car-following behavior of Lv1 and Lv2 AVs using the Wiedemann 99 model. In Table 1, findings regarding the standstill gap (CC0) and headway time (CC1) for AVs with Lv1 and Lv2 automation are summarized.

Through the comparison of the standstill gap (CC0), literature confirms that this parameter varies widely between studies, ranging from 6 to 0.5 m. The standstill distance is a parameter concerning an automated vehicle ability to travel with high precision. As a result, automation of driving should theoretically lead to shorter standstill distances [23]. Given that, most earlier studies consider CC0 as being the same or less than for manual driving (1.5 m) [16, 23, 26]. Yet, Zeidler et al.'s [25] work which analyzed empirical data from three Lv2 AVs prototypes shows that CC0 is usually underestimated. More recently, Goodall and Lan's [14] findings, which attempt to reproduce the driving behavior of a 2017 Audi Q7 with ACC, also corroborate bigger standstill gaps when compared to earlier literature. Overall, these findings suggest that the operational logic of the vehicles tested in Zeidler et al. [25] and Goodall and Lan [14] is not

Table 1: Standstill gap (CC0) and time headway (CC1) values for the Wiedemann 99 model.

Vehicle capability	CC0 (m)	CC1 (s)	Source
ACC	3.5	1.8	Goodall and Lan [14]
CACC	4.0	0.3/0.6/1.0	Zeidler et al. [25]
dCACC	6.0	1.0	
AV cautious	1.5	1.5	Sukennik et al. [16]
AV normal	1.5	0.9	
All knowing	1.0	0.6	
ACC	1.5	1.2	Rossen [26]
CACC	1.25	0.75	
Lv1	1.5	0.9	Atkins [24]
Lv2/3 cautious	2.5	1.8	
Lv2/3 normal cautious	2.0	1.2	
Lv2/3 normal assertive	1.0	0.8	
Lv2/3 assertive	0.5	0.6	
ACC aggressive	1.5	0.5	Bierstedt et al. [23]
ACC intermediate	1.5	0.8	
ACC conservative	1.0	1.2	

advanced as would be expected and thus does not allow to keep shorter gaps under stop-and-go traffic. Aside from that, the standstill distance in the Wiedemann 99 model is always a fixed value while the standstill distances of the empirical data vary [27].

Regarding the drivers' preferred time headway (CC1) in AVs, the existing literature is also not conclusive. In general, examples of the CC1 parameter indicate time headways similar to manual driving (0.9 s) or larger. Some authors speculate that this might be because people are not familiar with systems like ACC and hence prefer a more conservative configuration [28]. In addition, others further state that for transferring the driving task responsibility between the automated systems and the driver, AVs will most likely require longer time headways than in manual driving [29]. Still, this literature also sustains that CC1 can be significantly smaller. For instance, Zeidler et al. [25] stated that the systems used in their work allowed three different settings of the time headway: 0.3, 0.6, and 1.0 s. On the other hand, Goodall and Lan's [14] test vehicle had five time headway settings of 1, 1.3, 1.8, 2.4, and 3.6 s. Therefore, the differences in CC1 values found in this literature could be related to distinct development and deployment strategies used by manufacturers [30, 31].

The parameters that describe the following variation (CC2) and threshold for entering the "following" regime (CC3) of Lv1 and Lv2 AVs are presented in Table 2.

As for the following variation (CC2), the values found across the studies reviewed generally agree. For manual driving, a value of 4 m is frequently recommended [17]. However, unlike human drivers' stochastic behavior, automated driving is predictable and deterministic [8]. In other words, it implies fewer or even insignificant variations during automated driving, as corroborated by the CC2 values found in this literature.

Considering the threshold for entering the "following" regime (CC3), literature is once more ambiguous, with values ranging from −6 to −40 s. Essentially, CC3 is a measurement of the time elapsed while decelerating to reach the desired safety distance [21]. Hence, the wide range of findings might be due to differences in AVs' perceptual ability, precision, and reaction times [14]. Yet, it can be argued that a few examples of the CC3 parameter are greater than expected [23, 26]. For example, the CC3 parameter in Zeidler et al.'s [25] study is higher than the bounds often indicated by literature [−20, 0] [17]. However, the authors justified that it enables the tested vehicle to close smoothly during simulation.

The different values for the negative and positive "following" thresholds, CC4 and CC5, respectively, are summarized in Table 3 for Lv1 and Lv2 AVs.

The comparison of negative (CC4) and positive (CC5) "following" thresholds shows differences in the existing literature. Some studies support a setting equal to the default value used for simulating the human drivers' behavior (−0.35 and +0.35 m/s for CC4 and CC5, respectively) [23, 26]. Others, however, agree that when modeling AV's driving behavior, CC4 and CC5 can be greatly reduced [14, 16, 25]. Plausibly, it implies that oscillations during vehicle following can be small with little variation in comparison to human drivers [27].

Table 2: Following variation (CC2) and threshold for entering "following" (CC3) regime from the Wiedemann 99 model.

Vehicle capability	CC2 (m)	CC3 (s)	Source
ACC	2.0	−8	Goodall and Lan [14]
CACC	0.0	−40	Zeidler et al. [25]
dCACC	0.0	−40	
AV cautious	0.0	−10	Sukennik et al. [16]
AV normal	0.0	−8	
All knowing	0.0	−6	
ACC	3.0	−12	Rossen [26]
CACC	2.0	−12	
ACC aggressive	2.0	−8	Bierstedt et al. [23]
ACC intermediate	3.0	−12	
ACC conservative	4.0	−16	

Table 3: Negative (CC4) and positive (CC5) "following" thresholds for the Wiedemann 99 model.

Vehicle capability	CC4 (m/s)	CC5 (m/s)	Source
ACC	−0.1	0.1	Goodall and Lan [14]
CACC	0.0	0.0	Zeidler et al. [25]
dCACC	0.0	0.0	
AV cautious	−0.1	0.1	Sukennik et al. [16]
AV normal	−0.1	0.1	
All knowing	−0.1	0.1	
ACC	−0.35	0.35	Rossen [26]
CACC	−0.35	0.35	
ACC aggressive	−0.1	0.1	Bierstedt et al. [23]
ACC intermediate	−0.35	0.35	
ACC conservative	−0.6	0.6	

Table 4 shows the literature on the speed dependency of oscillation (CC6) and acceleration oscillation (CC7) for AVs with Lv1 and Lv2 driving automation.

The speed dependence of oscillation (CC6) is consistent across studies in the literature for AVs, with a value of zero. According to Bierstedt et al. [23], this is due to the fact that with driving technologies, the car can maintain a constant speed.

By contrast, there are several different values found for the acceleration during speed oscillation (CC7). Once again, part of this literature sustains a driving behavior similar to manual driving [14, 23]. However, research also demonstrates that when following other cars, AVs can use substantially lower accelerations/decelerations [16, 25, 26].

At last, in Table 5, we present the literature regarding the standstill acceleration (CC8) and acceleration at 80 km/h (CC9) for simulating Lv1 and Lv2 AVs.

Regarding the acceleration at standstill (CC8), the literature shows a range of values between 2 and 4 m/s^2 to reproduce AVs driving behavior. This shows quite some variation, which could be attributable to the different operational logics that manufacturers can implement. Nonetheless, some of these values might be unrealistic to represent the accelerations of real ACC systems. According to ISO 15622 : 2018, the average automatic acceleration for those systems shall not exceed 2 m/s^2 [30].

Table 4: Speed dependency of oscillation (CC6) and oscillation of acceleration (CC7) values for the Wiedemann 99 model.

Vehicle capability	CC6 ($10^{-4} rad/s$)	CC7 (m/s^2)	Source
ACC	0.0	0.36	Goodall and Lan [14]
CACC	0.0	0.25	Zeidler et al. [25]
dCACC	0.0	0.25	
AV cautious	0.0	0.1	Sukennik et al. [16]
AV normal	0.0	0.1	
All knowing	0.0	0.1	
ACC	0.0	0.25	Rossen [26]
CACC	0.0	0.1	
Lv1	0.0	0.25	Atkins [24]
Lv2/3 cautious	0.0	0.1	
Lv2/3 normal cautious	0.0	0.2	
Lv2/3 normal assertive	0.0	0.3	
Lv2/3 assertive	0.0	0.4	
ACC aggressive	0.0	0.4	Bierstedt et al. [23]
ACC intermediate	0.0	0.25	
ACC conservative	0.0	0.1	

Table 5: Standstill acceleration (CC8) and acceleration at 80 km/h (CC9) values for the Wiedemann 99 model.

Vehicle capability	CC8 (m/s^2)	CC9 (m/s^2)	Source
ACC	2.0	1.17	Goodall and Lan [14]
CACC	3.5	1.0	Zeidler et al. [25]
dCACC	3.5	1.5	
AV cautious	3.0	1.2	Sukennik et al. [16]
AV normal	3.5	1.5	
All knowing	4.0	2.0	
ACC	3.5	1.5	Rossen [26]
CACC	3.5	1.5	
Lv1	3.5	1.5	Atkins [24]
Lv2/3 cautious	3.2	1.2	
Lv2/3 normal cautious	3.4	1.4	
Lv2/3 normal assertive	3.6	1.6	
Lv2/3 assertive	3.8	1.8	
ACC aggressive	4.0	2.0	Bierstedt et al. [23]
ACC intermediate	3.5	1.5	
ACC conservative	3.0	1.0	

In terms of AVs acceleration at 80 km/h (CC9), literature varies again. The recommended value for simulating the manual driving behavior is 1.5 m/s^2. Values above are frequently related to an aggressive driving rationale, and values below are associated with a conservative/cautious logic.

Overall, this literature highlights that most parameters of the Wiedemann 99 model vary considerably between studies. Several aspects inherent to these cars' development and deployment strategies make the following behavior a complex phenomenon that is hard to predict. Accordingly, in future research, the emerging driving behavior of AVs should be addressed for different manufacturers, levels of driving automation, and traffic conditions since it will allow the development of more appropriate car-following models.

2.3. Parameter Estimation Method. It is well known that the methodology behind these model parameters estimation is of extreme importance to the confidence level of the whole study. Table 6 presents the methods used to estimate the W99 model parameters previously discussed for AVs with Lv1 and Lv2 autonomy.

Based on this literature review, we conclude that researchers have used different methods to reproduce the longitudinal driving behavior of AVs. Since PTV Vissim was one of the first tools giving some steps towards preparing their software for simulating AVs [17], early studies have adjusted the Wiedemann model parameters based on theoretical assumptions about the effects of automation on vehicle driving behavior [23, 24, 26]. This is plausible since new technologies tend to be costly when deployed in the market and thus are not immediately available to be extensively tested.

More recent studies have made an effort to collect empirical data in order to adjust the Wiedemann model parameters. In this sense, Zeidler et al. [25] adjusted and validated some of the Wiedemann model parameters within PTV Vissim to match the derived characteristics of the tested vehicles, while Sukennik [16] used empirical data to develop several driving logics for different forms of AVs. However, in both cases, data were obtained in a test track rather than under real traffic situations. Only the study from Goodall and Lan [14] collected empirical data under real traffic situations from which authors measured four model parameters directly from the field observations of the test vehicle.

Overall, more efforts should be devoted to the collection of empirical evidence as the driving logics of these vehicles vary widely, both in capability as well between manufactures. More importantly, this literature does not provide a methodology that can be used by other

Table 6: Methods for estimating the Wiedemann 99 model parameters for AVs with Lv1 and Lv2 autonomy.

Source	Data	Parameter estimation
Goodall and Lan [14]	Field experiments were conducted under real traffic situations using a 2017 Audi Q7 assisted by the ACC functionality.	Parameters of the Wiedemann 99 model were measured directly from the field observations of the test vehicle.
Zeidler et al. [25]	Based on the data collected in the CoExist project [27].	The Wiedemann 99 parameters in PTV Vissim were adjusted to match the derived characteristics of both automated cars tested.
Sukennik et al. [16]	Field experiments were conducted on a test track using 2 Toyota Prius cars. One had equipped the CACC functionality, while the other had the dCACC functionality.	The Wiedemann 99 parameters in PTV Vissim were adjusted to reproduce three driving logics for AVs based on the derived characteristics of the cars tested.
Rossen [26]	No trajectory data were collected in this study.	The driving behavior of AVs was simulated in PTV Vissim based on the assumptions and parameter values found in earlier literature.
Atkins [24]	No trajectory data were collected in this study.	The authors modified the existing Wiedemann 99 model parameters within PTV Vissim to reproduce several forms of AVs based on their knowledge of early ACC and CACC systems.
Bierstedt et al. [23]	No trajectory data were collected in this study.	The authors modified the existing Wiedemann 99 model parameters within PTV Vissim to develop conservative, intermediate, and aggressive ACC characteristics.

researchers in order to adjust the parameters from the Wiedemann 99 car-following model based on empirical data from AVs. This forms an important gap in the existing literature, which is the main contribution of this study. We do hope to inspire the transport planning community to perform analysis similar to the work presented in our paper for different brands and forms of automated driving technologies.

3. Data Collection and Preparation

Car-following models are studied on the basis of high-quality trajectory data. Over the years, different approaches or methods have been developed to collect such trajectory data in transportation studies [32]. A review of existent literature reveals that the research community has centered its attention on the collection of naturalistic driving data (NDD) [18, 25, 33]. These are experimental methods for collecting unobtrusive data and typically aim to understand the driving behaviors adopted in their daily activities over long periods of time. Distinctly, the experiment in this study is a controlled on-road experiment on a fixed route and of short duration according to the definition of Carsten et al. [34]. This Section describes the pilot study conducted and presents the extraction methodology of the car-following events collected.

3.1. Pilot Study. This study used vehicle trajectory data collected in Coimbra, Portugal, for ten consecutive days during June 2017. A total of two roadway sections were selected, one freeway and one expressway. The freeway is a 5 km section of IC2 with two lanes per direction between the Fornos and Ponte Açude interchanges. Throughout this section, the maximum legal speed varies between 80 km/h and 100 km/h. The expressway is a 5 km long section in Via Rápida de Taveiro also with two lanes in each direction between Ponte Açude and Taveiro interchanges. The maximum legal speed ranges from 80 km/h to 90 km/h. The existence of on-ramps and off-ramps at the end of each section has facilitated the reversal maneuvers and materialized a continuous circuit as shown in Figure 3. Depending on the traffic density and desired speed, a lap to the experiment circuit could take around 15 to 25 minutes. Furthermore, all sessions were conducted under good weather conditions and during day time.

A Mercedes-Benz E-Class 350d station wagon of the year 2017 was instrumented (see Figure 4). This vehicle driving technology includes a Driving Assistance Package to assist the human driver in adapting the vehicle speed, controlling distance, lane keeping, steering, and lane changing in specific scenarios. However, the latter was unavailable in conformity with the Portuguese legislation. During the pilot study, the level of driving automation was level 2, according to SAE International [2]. A data logger device (DL1 Club) from Race Technology was equipped in the probe vehicle to store and synchronize all data collected. The built-in high accuracy GPS antenna and accelerometers enabled recording speeds, accelerations, and geographical positions. In addition, two cameras were installed to validate the sensor-based findings, observe the driving behavior, and determine the relative distance to the leading vehicle. All instrumentation was mounted to be as unobtrusive as possible (see Figure 4).

Vehicle trajectory data were extracted from the data logger using the Race Technology Analysis software. The database obtained contains information on recorded speeds, accelerations, following distances, and geographical positions.

Since drivers could regulate the desired speed and target headway settings during the automated operation of the vehicle, it was fundamental to perform the experiment with a number of different individual participants to capture their individual preferences. Based on a survey designed and distributed by the University of Coimbra

Figure 3: Experiment route in the city of Coimbra, Portugal: (a) circuit map; (b) IC2 freeway; and (c) via Rápida de Taveiro; (screenshots from Google Maps).

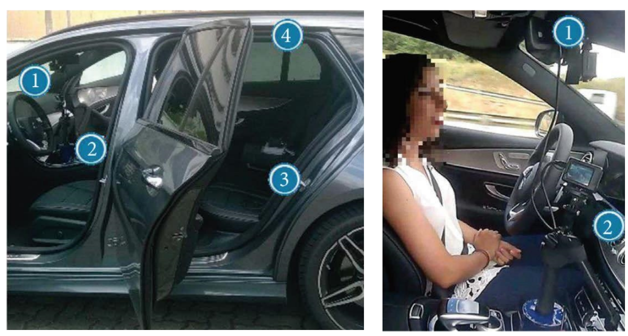

Figure 4: Installed equipment: (1) video camera recording the traffic in front; (2) video camera recording the vehicle interior and dashboard; (3) datalogger; (4) GPS antenna.

population, these were selected according to the following criteria: reside in Coimbra for at least one year—this guaranteed that drivers had the necessary knowledge of the area, where tests occurred; hold a driving license for three or more years; and to allegedly drive on a daily basis—assuring an experienced sample of drivers. Before the experiment, all selected participants completed an informed consent form. Their ages ranged from 25 to 66 years old, with a mean value of 44.50 and their driving experience varied between 1 and 47 years (mean = 23.04). Following that was provided to each participant a description and demonstration session of the instrumented car technology in accordance with the manufacturer instructions. Participants were also informed that the instrumented car systems had limitations and that they should intervene whenever necessary. In accordance with previous research, a familiarization session (at least 10 km) was conducted to allow participants to drive as naturally as possible before the experiment [35]. It took place on a road near the experiment's circuit. Then, with one researcher sitting in the passenger seat to provide unavoidable guidance regarding the route and operation of the automated systems, participants were requested to complete one lap while driving manually and four with the Lv2 systems engaged.

Finally, all data gathered were collected by a random sample of 26 licensed Portuguese drivers who, all together, traveled 2600 km during the study period.

3.2. Car-Following Period Extraction. All data hereon analyzed were obtained during four laps with the Lv2 systems engaged. Situations of disturbance have been initially identified and excluded from our dataset based on visual observations of the cameras' data to, desirably, consider only potential car-following events deemed representative of the pilot study general driving conditions [36]. In this study case, the most recurrent perturbations include, among others, accidents in the circuit road, drivers regaining control over the vehicle to take phone calls, and data from the participants circulating outside the circuit. After that initial extraction step, only car-following events that fulfilled the following criteria remained eligible for further analysis [18, 25]:

(i) Duration of the car-following event is longer than 15 s.

(ii) Following and lead vehicles were driving in the same lane with a range less than 120 m.

(iii) Automated driving mode was switched on and working.
(iv) The system was not overridden by the human driver.
(v) The following procedure was not interfered by another vehicle cutting in.

In total, 61 car-following events were extracted and represented about 22 minutes of automated driving. At last, all events analyzed in this study correspond to a car following another car. Figure 5 depicts a typical car-following event.

4. Calibration and Validation Methodology

Model calibration is a procedure that systematically estimates optimal parameters in order to adapt a given car-following model to an observed behavior as accurately as possible. Optimization methods have been vastly applied in numerous studies to solve such calibration problems [37]. In this Section, we describe the calibration of the Wiedemann 99 car-following model based on optimization methods and which comprised defining an objective function, establishing parameter constraints, applying a collision penalty, adopting an integration scheme, and selecting an optimization algorithm. At last, we also describe the validation procedure.

4.1. Objective Function. Normally, the objective function defines if the difference between the simulated and observed measures of performance (MoPs) is to be minimized or maximized subject to a set of parameters. To this end, the mathematical form of the objective function consists of two fundamental components: the measures of performance (MoPs) and goodness of fit (GoF) function.

MoPs are considered a metric that illustrates a particular car-following behavior. The temporal headways [38, 39], following distance [40, 41], and following vehicle speeds [42, 43] are frequently used metrics in previous studies. However, several authors [43, 44] provide substantial evidence that supports using the following distance over other metrics. Basically, minimizing the following distance error does not jeopardize other metrics' accuracy, while the contrary is not always true [11].

On the other hand, the GoF function evaluates the performance of the calibration solution. For example, the Mean Absolute Error (MAE) [45] or Theil's inequality coefficient (U) [46] are some of the statistics employed by researchers to estimate the fitness between simulated and observed MoPs. However, the root mean square error (RMSE) is the most commonly selected GoF function in car-following calibration [40] because it is very sensitive to extra large and small values [47].

Hence, in this study, we use a single-objective function set as an RMSE of the following distance (S front edge to rear-end) given according to

$$\text{RMSE of the following distance} = \sqrt{\frac{1}{N}\sum_{i=1}^{N}\left(S_i^{sim} - S_i^{obs}\right)^2}, \tag{10}$$

where S_i^{sim} and S_i^{obs} are the simulated and observed following distances at time step i and N is the number of observations. In short, the outlined objective function will find the values of the adjustable parameters from the W99 model that minimize the RMSE while staying within constraints.

4.2. Parameter Constraints and Collision Penalty. Another crucial part of the calibration procedure involves defining constraints to a set of calibration parameters. More specifically, it requires defining minimum and maximum values to those parameters from the W99 car-following model that are not measured easily based on empirical data. Therefore, the constraint term refers to logical boundaries that a solution to an optimization problem must satisfy [48]. Table 7 presents the physical meanings and boundaries of all parameters that are adjustable in the model calibration.

It should be noted that the car-following model of Wiedemann uses follower-leader pairs for the calculation of several driving behavior parameters (CCX), threshold values, regime values, and functions. Since the parameter VDES pertains to the vehicle behavior under free driving circumstances, it is thus impossible to estimate it from such data. However, with the advent of Lv2 driving automation, the user must select a target speed setting for the vehicle automated operation, which in our study's case is known based on the video recordings from the car dashboard. But, because most vehicles display an overestimated speed of travel in the dashboard, VDES was estimated during the calibration process (see Figure 2) with a ±5 km/h deviation from the observed value.

Additionally, we have to take into account that some combinations of parameters may result in possible collisions. In practice, it further implies adding a large penalty term to the objective function, which will make these solutions unattractive to the optimization algorithm [49].

4.3. Integration Scheme. In such calibration problems, the follower-leader behavior is investigated at each time instant [50]. The leader vehicle acceleration, speed, and position are updated using empirical observations. In turn, the following vehicle acceleration is governed by the W99 car-following model while speed and position are updated using standard integration schemes such as the Forward Euler method [51]. The latter scheme is used in this study to calculate the continuous motion of the following vehicle (denoted as n) and is as written in equations (3) and (4):

$$V_n(t + \Delta T) = V_n(t) + a_n(t) \times \Delta T, \tag{11}$$

$$X_n(t + \Delta T) = X_n(t) + V_n(t) \times \Delta T, \tag{12}$$

where V_n and X_n are the speed and position, respectively, a_n is the acceleration calculated by the Wiedemann 99 car-following model, t is the corresponding time instant in seconds, and ΔT is the update time step.

4.4. Optimization with Genetic Algorithm. Several optimization algorithms like the downhill simplex [52], OptQuest

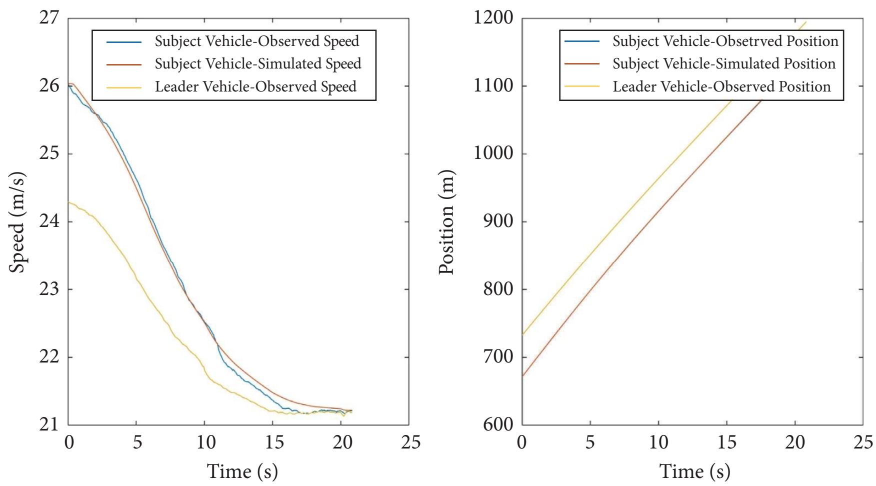

FIGURE 5: Speed and position curves from a typical car-following event.

TABLE 7: Calibration parameters of the Wiedemann 99 car-following model.

Parameters (unit)	Short description	Bounds
CC0 (m)	Standstill gap	[0, 20]
CC1 (s)	Headway time	[0, 5]
CC2 (m)	Following variation	[0, 10]
CC3 (s)	Threshold for entering "following"	[−20, 0]
CC4 (m/s)	Negative "following" threshold	[−5, 0]
CC5 (m/s)	Positive "following" threshold	[0.1, 5]
CC6 $(10^{-4} rad/s)$	Speed dependency of oscillation	[0.1, 20]
CC7 (m/s^2)	Oscillation acceleration	[−1, 1]
CC8 (m/s^2)	Standstill acceleration	[0, 8]
CC9 (m/s^2)	Acceleration at 80 km/h	[0, 8]
VDES (km/h)	Desired speed of following vehicle	[1, 150]

Multistart [46], Deep Reinforcement Learning [53, 54], and Genetic Algorithm [55] have been implemented and compared in the field of car-following calibration. Among alternatives, the Genetic Algorithm (GA) is the most suitable optimization method because it is particularly useful to solve nonlinear problems with a complex search space (as in this study case) while increases the probability of finding a global rather than local optimum [18]. Therefore, the GA was used in this study to find optimal calibration parameters that minimize the objective function in equation (2). The optimization routine consists of creating successive generations of individuals based on the principles of evolution and natural selection. Although the problem seems simple enough, it is a demanding optimization procedure that includes six iterative steps: (1) initialization; (2) fitness assessment; (3) selection; (4) crossover; (5) mutation; and (6) convergence. For a comprehensive introduction on the subject, we refer readers to Holland [56] and Spall [57]. In Table 8, the relevant settings of our GA are described for future reference.

Because the GA is a stochastic global optimization procedure, it finds slightly different solutions in each optimization run. Consequently, to find a solution close to the global optimal, the proposed optimization routine has been repeated a total of 10 times for each car-following event. Finally, the set of parameters that resulted in the minimum error (i.e., RMSE) was selected.

4.5. Validation. Unlike calibration, validation is a simple task that aims to reproduce specific car-following events by using parameters independently calibrated. This study applies a k-fold cross-validation framework to test the reproducing accuracy of our calibrated parameters. This method reduces the likelihood of bias while allowing all available data to be used [58]. Specifically, the following logic was applied:

Step 1. The entire car-following database was divided randomly into k near equal sets, also known as folds.

Step 2. We use $k-1$ folds as the calibration set, and the resulting calibrated parameters are used on the basis of the remaining kth fold to conduct the validation. Record the validation error (i.e., RMSPE).

Step 3. We repeat this process until each k-fold has been used as the validation set.

Step 4. To finalize, we take the average of all recorded error scores.

Hence, our database was divided into 5-folds. A variant of the root mean square percent error (RMSPE) was adopted to estimate the difference between the simulated and observed following distance (S) during validation. This statistic provides information about the magnitude of relative errors and was selected to allow comparing the obtained validation errors with similar studies [18]. The RMSPE is given by

$$\text{RMSPE of the following distance} = \sqrt{\frac{\sum_{i=1}^{N}\left(S_i^{sim} - S_i^{obs}\right)^2}{\sum_{i=1}^{N}\left(S_i^{obs}\right)^2}}, \tag{13}$$

Table 8: Description of the genetic algorithm settings according to MATLAB.

Algorithm settings	Value/method	Short description
Population size	500	Specifies how many individuals there are in each generation.
Maximum generations	800	Defines the maximum number of iterations for the GA to perform.
Stall generations	150	Calculates the weighted relative change in the objective function value over stall generations.
Fitness scaling	Rank	Function that scales and sorts individuals based on the values of the objective function.
Parent selection	Stochastic	Function that selects parents for the next generation based on their scaled values.
Children reproduction	Elite and crossover	Selects elite (0.05) and crossover (0.8) children for the next generation. Rest of the children are produced by mutation operations.
Crossover	Scatter	Indicates how two individuals form a crossover child for the next generation.
Mutation	Gaussian (mean 0)	Indicates how two individuals form a mutation child for the next generation.
Tolerance function	1×10^{-6}	Exit criteria.

where S_i^{sim} and S_i^{obs} are the simulated and observed following distances at time step i and N is the number of observations in each car-following event.

5. Results and Analysis

This Section presents the estimated parameters from the Wiedemann 99 car-following model in respect to the driving behavior of a Mercedes-Benz with level 2 driving automation. In particular, subsection 5.1 describes the assumptions and simplifications made. Subsection 5.2 analyzes the estimates of all calibration parameters, and to conclude, subsection 5.3 reports the validation error. All tasks were coded and performed using the R2020b release of MATLAB.

5.1. Assumptions and Simplifications. In order to reproduce the driving behaviors observed in our data through the Wiedemann 99 car-following model and to reduce complexity, it was necessary to make a number of assumptions and simplifications.

As there were no stopped traffic situations observed during our pilot study, the values for **CC0** and **CC8** parameters were not possible to be derived from the available data. **CC0** is the standstill gap that the following vehicle keeps behind a leading vehicle when both are at stationary positions and **CC8** is the desired acceleration of the follower vehicle when starting from standstill [17]. A default value for both parameters, **CC0** (1.5 m) and **CC8** (3 m/s^2), was used according to the most recent literature on the subject for vehicles with Lv2 systems [16].

Furthermore, such literature has shown that given the deterministic behavior of AVs and to reflect much smaller oscillation during the following procedure, the **CC2** and **CC6** driving parameters should take the value of zero [16]. **CC2** is the following variation in meters, and a value of zero results in a relatively stable following process [17]. **CC6**, namely, the speed dependency of oscillation when assumes value zero, indicates that the following distance does not influence the speed oscillation during the "following" regime [17]. In Table 9, we review the default values adopted for the model parameters described above.

Additionally, the **CC9** parameter denotes the acceleration of a vehicle when at 80 km/h [17]. However, since most of the car-following events analyzed have occurred at speeds beyond 80 km/h, **CC9** was estimated based on an independent analysis of our data. Strictly speaking, it entailed estimating **CC9** as the mean of the maximum acceleration rates of a vehicle moving at 80 km/h, which is a recurrent approach in literature [14, 22]. Table 10 presents the estimates of this parameter.

5.2. Estimates of W99 Parameters. Considering all assumptions and simplifications made, the calibration parameters in this study are **CC1**, **CC3**, **CC4**, **CC5**, **CC7**, and **VDES**. The Wiedemann 99 car-following model was independently calibrated and validated five times. Results are presented in Table 10, quantifying the mean, standard deviation, and range (5th and 95th percentiles) of the estimated parameters aggregated across the five iterations of cross-validation.

The calibration error (RMSE) achieved between the simulated and observed following distance was found to be on average 0.17 m. This shows that for each car-following event investigated, the genetic algorithm has approximated the observed following distance with reasonable accuracy. The cumulative distribution curves for each parameter are presented in Figure 6 to, hopefully, enrich the existing knowledge about the following behavior of automated vehicles, particularly from those with level 2 driving systems. Finally, we analyze the estimates obtained for each parameter more closely.

CC1 is the time headway between two vehicles, in other words, the distance in seconds which a driver wants to maintain at a certain speed from a leader vehicle. At an individual level, this parameter captures the preferred distance headway setting of each user. According to the literature, values above default (0.9 s, used for vehicles with no automation) imply a cautious driving behavior, which is the case of our estimates for automated driving (1.48 s) [17]. Plausibly, this result suggests that drivers have selected a larger headway setting for the Driving Assistance Package than is typically maintained during manual driving. This behavior is reasonable, partially because the minimum headway setting of the Driving Assistance Package is more conservative than when driving manually [59] and partially because these systems require somewhat longer headways in

Table 9: Default parameters to simulate Lv2 AV behavior using the Wiedemann 99 model.

Parameters (unit)	Value	Explanation*
CC0 (m)	1.5	Default value in PTV Vissim for AV cautious.
CC2 (m)	0.0	Default value in PTV Vissim for AV cautious.
CC6 ($10^{-4}rad/s$)	0.0	Default value in PTV Vissim for AV cautious.
CC8 (m/s^2)	3.0	Default value in PTV Vissim for AV cautious.

*Adopted based on CoExist report [16].

Table 10: Estimated parameters from Wiedemann 99 car-following model for Lv2 AVs.

Parameters (unit)	Mean	Median	Std. Dev.	5%	95%
Parameters estimated by calibration					
CC1 (s)	1.48	1.46	0.40	0.97	2.07
CC3 (s)	−6.73	−6.26	2.78	−11.59	−3.73
CC4 (m/s)	−0.16	−0.08	0.21	−0.56	−0.01
CC5 (m/s)	0.17	0.15	0.07	0.11	0.29
CC7 (m/s^2)	0.13	0.12	0.10	0.03	0.29
VDES (km/h)	98.85	99.29	7.60	88.89	112.11
Parameters individually estimated based on physical meaning					
CC9 (m/s^2)	1.03	0.97	0.38	0.63	1.84

order to transfer the vehicle control for the driver with safety [26]. The time headway (**CC1**) is one of the most important parameters in the Wiedemann 99 car-following model in terms of link capacity. Consequently, as the headway between vehicles increases, the resulting route capacity of any transit system is expected to decrease.

The **CC3** parameter represents the time elapsed in seconds from the start of the deceleration process to the beginning of the "following" regime. The default value is −8.00 s (for Lv0 vehicles) [17]. In this study, the estimated value was −6.73 s, which indicates that AVs such as the one investigated take less time to perceive and react to a slower leader vehicle. This result is a plausible driving behavior for any AVs because these rely on systems developed to perceive and react much faster than human drivers [60]. Empirically, **CC3** can influence a specific lane flow distribution though its effects become insignificant with increasing traffic volumes [61].

CC4and **CC5** control the maximum negative and positive speed variations during the "following" regime, respectively. PTV Vissim [17] manual suggests that these parameters should have the same magnitude and opposite signs, which indicates symmetry between the vehicle acceleration and deceleration behavior. The default values for **CC4** and **CC5** are −0.35 m/s and +0.35 m/s, respectively (for manual vehicles). Interestingly, our estimates are −0.16 m/s and +0.17 m/s, for **CC4** and **CC5**, respectively. In general, values closer to zero suggest a faster response from the following vehicle to changes in the speed of the leading vehicle, which is a characteristic foreseen in the driving behavior of AVs [16]. The slightly differing (module) values of **CC4** and **CC5** further indicate that the automated vehicle under investigation is more sensitive to the leader vehicle deceleration than to its accelerations during the "following" regime. This behavior is logical since these vehicles' development and deployment strategies should focus on enhancing traffic safety.

CC7 represents the actual acceleration rate in the "following" regime that causes the oscillation in relative speed. This parameter has a default value of 0.25 m/s^2 (estimated for vehicles with no automation) [17]. However, our estimates for automated driving reveal a lower value of **CC7** (0.13 m/s^2). Due to that, we can argue that the probe vehicle has a low acceleration/deceleration profile during the "following" regime, perhaps to maintain a specific headway setting at almost zero relative speed.

VDES is the desired speed that drivers wish to travel under unconstrained traffic situations [16]. At an individual level, this parameter captures the desired speed setting selected by each user. To properly analyze our sample desired speed settings of the Driving Assistance Package, we exhibit in Table 11 the calibration results by roadway type.

The maximum legal speeds allowed in the expressway range between 80 km/h and 90 km/h. However, our estimates show that, on average, drivers have selected a higher speed setting during automated driving. Similar behavior was found throughout the freeway, where the speed distribution varies between 80 km/h and 100 km/h. Overall, these findings indicate that drivers have chosen to travel at speeds that exceed the current speed limits in force. This trend is persistent in the driving behavior of Portuguese drivers, as previous studies concerning manual driving sustain [62]. Another reason could be due to automation complacency. For example, drivers did not change the setting of the automated driving system in a speed limit violation scenario, thereby allowing the vehicle to drive above the posted speed limit [4]. In addition, the standard deviation estimates support considerable behavioral differences between individual drivers. Nonetheless, the distribution function of desired speeds is of particular importance since it affects link capacity and achievable travel times [16].

5.3. Validation of W99 Parameters. In the validation phase was employed a five-fold cross-validation framework to compare the observed following distance for each car-following event in the kth set, with that simulated by using the

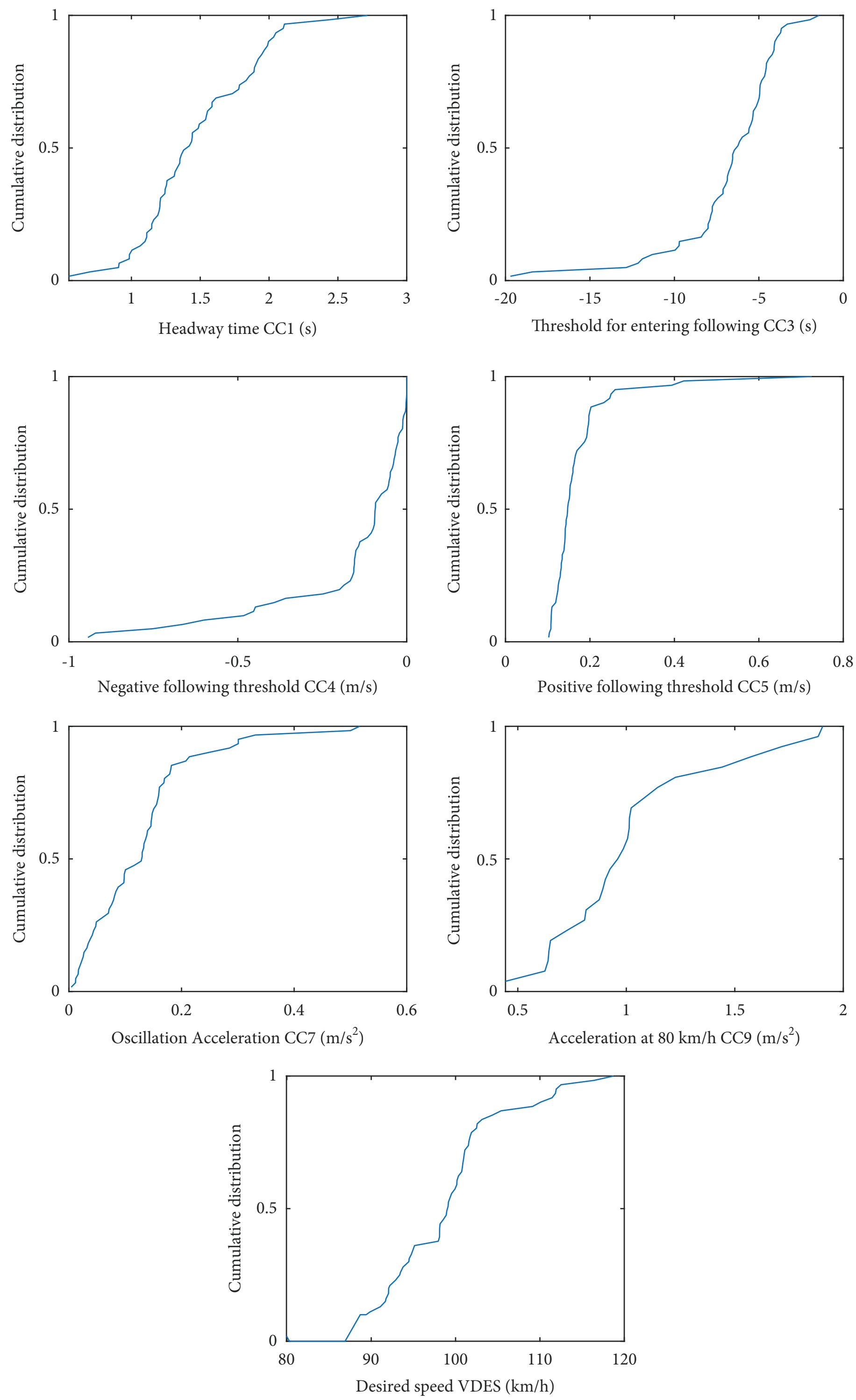

Figure 6: Cumulative distribution of parameter estimates for the Wiedemann 99 car-following model.

average value of the parameters calibrated in $k-1$ sets. The validation error (RMSPE) obtained across all five folds was on average 20%, indicating a feasible reproducing capacity of the calibration parameters reported in this study. It is worth noticing that the W99 model produced one collision during the validation phase.

Table 11: Desired speeds per roadway type.

VDES (km/h)	Mean	Median	Std. Dev.	5%	95%
Expressway	95.68	94.90	7.01	81.76	105.24
Freeway	100.91	100.52	7.25	89.50	113.47

Table 12: Summary of our estimates for Lv2 AVs and Vissim default values.

Parameters (unit)	Lv2 AVs	Vissim default values
CC0 (m)	1.50*	1.50
CC1 (s)	1.48	0.90
CC2 (m)	0.00*	4.00
CC3 (s)	−6.73	−8.00
CC4 (m/s)	−0.16	−0.35
CC5 (m/s)	0.17	0.35
CC6 ($10^{-4} rad/s$)	0.00*	11.44
CC7 (m/s^2)	0.13	0.25
CC8 (m/s^2)	3.00*	3.50
CC9 (m/s^2)	1.00**	1.50

*Default values adopted based on CoExist report [16]. **Parameters individually estimated based on physical meaning.

6. Discussion and Conclusions

The purpose of this study was to define and test a methodology to incorporate the driving behavior of automated vehicles in the Wiedemann 99 car-following model, whose results may be applied to future modeling efforts.

We introduced modifications in the equations of the Wiedemann 99 model, which is a well-known psycho-physical car-following model, to reproduce the expected behavior of AVs. This modified version was implemented into a calibration framework and formulated as an optimization problem that used a genetic algorithm to find optimal values of the model parameters. The optimization function was simply the error minimization between the following distance values simulated in the Wiedemann model and the following distance values directly observed from empirical data.

A pilot study was recently conducted in Coimbra, Portugal, to collect trajectory data from the longitudinal driving behavior of an automated vehicle assisted with level 2 driving automation. In total, 61 car-following events were used to support the calibration and validation tasks. We found that the following distance calibration errors are on average 0.17 m (RMSE). This result is consistent with the errors reported in previous studies [38, 44, 46] and sustains the W99 model descriptive capability to simulate Lv2 AV's following behavior with no significant deviations from the observed trajectories. In the validation phase, the following distance error was found to be 20% (RMSPE) and is also in line with the estimates from earlier studies [18, 63]. This result further indicates that our calibrated parameters can reproduce the dynamic behavior of Lv2 AVs with reasonable consistency and robustness.

Given all assumptions and simplifications regarding the Wiedemann 99 model, this study's calibration parameters are **CC1**, **CC3**, **CC4**, **CC5**, **CC7**, and **VDES**. Additionally, the **CC9** parameter was individually estimated based on its physical meaning. Table 12 compares our study findings to the recommended values for human-driven vehicles in Vissim.

Essentially, our parameter estimates demonstrate a distinct driving behavior from human drivers and are to a great extent consistent with some of the trends found in AVs literature. However, there are a few exceptions that support differences related to automated vehicles, operational logic, perception ability, and reaction times.

For instance, the time headway (**CC1**) estimates indicate a cautious driving behavior, which is partially corroborated in Atkins [24] and Sukennik [16]. However, several authors state that some AVs can also adopt aggressive driving behaviors or driving behaviors similar to human drivers [23–25].

Our findings related to the **CC3** parameter, threshold for entering the "following" regime, are consistent with values documented for vehicles equipped with Automated Driving Systems (SAE Lv3 or higher) [16]. This result is plausible because due to the fast technological progress, some vehicles today can already offer advanced Lv2 systems, which is the case of the Driving Assistance Package included in this study vehicle.

CC4 and **CC5** are the maximum negative and positive speed variations during the "following" regime, respectively. In general, both parameters show a quite sensitive behavior to changes in the speed of the leading vehicle when compared to the values in Bierstedt et al. [23] and Rossen [26]. However, our estimates suggest a slightly less sensitive behavior than those described in Sukennik [16] and Goodall and Lan [14]. At last, we have found that differences exist between these parameter values. Explicitly, **CC4** is more sensitive to the leader vehicle than **CC5**, which is a new finding.

CC7 represents the vehicle acceleration during speed oscillations. The bulk of AVs literature, in particular, regarding Lv2 or similar systems (i.e., adaptive cruise control) evidences values higher than our estimates [14, 24–26] and in some cases even for Lv5 AVs [64]. Perhaps, certain assumptions are made that impact the driving behaviors of AVs to be similar to human driving. Only Sukennik's [16] work, which is based on a small-scale study conducted in a test track with an Lv2 Toyota Prius prototype, supports our results.

The **CC9** parameter is the acceleration of a vehicle when at 80 km/h. Our results are in line with the findings in Sukennik [16] and Goodall and Lan [14] and sustain that AVs similar to the one tested (Lv2 Mercedes-Benz E-Class of 2017) have a less aggressive acceleration profile when compared with manual driving.

VDES is the desired speed distribution from our sample of drivers, where the 5th percentile $VDES05 = 89$ km/h, the 50th percentile $VDES50 = 99$ km/h, and the 95th percentile $VDES95 = 112$ km/h. Overall, this result shows that there-exists significant differences in the desired speed settings of the Driving Assistance Package among drivers. This result is plausible and is a typical behavior often reported in studies regarding manually driven vehicles [20].

Overall, besides providing a methodology to incorporate automated driving in the Wiedemann 99 car-following model, this paper also enriches existing literature in relation to the driving behavior of Lv2 AVs based on empirical data. Aside from that, this methodology's results are relevant to transportation planning in the sense that it offers useful insights on how including specific driving behaviors in microscopic traffic simulation tools such as in PTV Vissim can shape the dynamics of our transportation networks in the decades to come.

For instance, our findings sustain that Lv2 AVs keep a larger time headway (**CC1**) when compared to manual driven vehicles and hence are more likely to decrease our transport infrastructure capacity. From an traffic engineer's view point, this is not desirable since it might result in a poor traffic performance in terms of flow, speed, and delay time.

On the other hand, since Lv2 AVs keep higher gaps from the vehicle in front and unlike human-driven vehicles they continuously attempt to keep a constant speed corroborated by **CC4**, **CC5,** and **CC7** estimates, it is expectable that their effects on the traffic safety are likely positive.

6.1. Limitations and Directions for Future Research. Developing and testing a methodology to incorporate the driving behavior of automated vehicles in the Wiedemann 99 car-following model is a challenging multifaceted task. As such, in order to carry out this research, various assumptions and simplifications have been made.

One of the major limitations of this study is related to data collection; in particular, our experiment procedure did not include stopped traffic situations which are required to estimate some parameters from the Wiedemann 99 model. Therefore, we suggest the inclusion of such situations in future research.

Another limitation is that our findings are derived based on a small-scale pilot study, which implies that this method's results cannot be generalized to wider society. However, given that new vehicular technologies are arriving in the market at a fast pace, we recommend using this method because it provides valid insights about the driving behaviors observed under real traffic conditions and guidance for future research. Large-scale naturalistic studies should be employed, including a representative sample of drivers, different vehicle brands, distinct forms of driving automation, large spatial coverage, and mixed traffic conditions, and over long periods.

A limitation of this study's methodology is that it was not developed to capture the control transition between the human driver and the automated driving systems. Instead, we provide a methodology to capture the longitudinal automated operation of production vehicles. Despite its complexity, future research should also consider this mechanism to allow a more realistic characterization from the driving behavior of different generations of automated vehicles.

At last, confounding factors related to AV performance should be also taken into consideration in future research. Failing to account for these may contribute to accidents, systematic bias, and measurement errors. At the same time, it can even explain differences between similar studies. That being said, one should note that different forms of driving automation impose distinct confounding factors. In our pilot study case, confounding factors were controlled to minimize their impact on the probe vehicle performance. These were (a) the weather conditions — Lv2 driving tech has several technical limitations that limit its operation under snow, fog, and rain conditions; (b) road marks — the probe vehicle automated operation relies upon visual input; and (c) traffic characteristics appropriated for the capability of the automated systems — available Lv2 tech can only operate in highways or similar roads.

Data Availability

This study's database is available from the corresponding author upon request.

Conflicts of Interest

The authors declare that they have no conflicts of interest.

Acknowledgments

This study was partially funded by ARDITI-Regional Agency for the Development of Research Technology and Innovation through the Ph.D. Scholarship with Reference M1420 Project 09-5369-FSE-000001 and by FCT-Portuguese Foundation for Science and Technology through the Ph.D. Scholarship with Reference 2021.05617.BD. The authors would like to especially thank Mercedes-Benz for providing a vehicle and workshops. The authors would also like to thank all the participants and staff involved in this study.

References

[1] S. A. Bagloee, M. Tavana, M. Asadi, and T. Oliver, "Autonomous vehicles: challenges, opportunities, and future implications for transportation policies," *Journal of modern transportation*, vol. 24, no. 4, pp. 284–303, 2016.

[2] Sae International, "J3016_201806 taxonomy and definitions for terms related to driving automation systems for on-road motor vehicles. Technical report," *SAE International*, 2018, https://www.sae.org/standards/content/j3016_201806/.

[3] R. Rodrigues, F. Moura, A. Bastos Silva, and Á. Seco, "The determinants of Portuguese preference for vehicle automation: a descriptive and explanatory study," *Transportation Research Part F: Traffic Psychology and Behaviour*, vol. 76, pp. 121–138, 2021.

[4] A. Várhelyi, C. Kaufmann, C. Johnsson, and S. Almqvist, "Driving with and without automation on the motorway–an observational study," *Journal of Intelligent Transportation Systems*, vol. 25, no. 6, pp. 587–608, 2020.

[5] H. Furey and S. Hill, "Mit's moral machine project is a psychological roadblock to self-driving cars," *AI and Ethics*, vol. 1, no. 2, pp. 151–155, 2020.

[6] D. Milakis, "Long-term Implications of Automated Vehicles: An Introduction," *Transport Reviews*, vol. 39, no. 1, pp. 1–8, 2019.

[7] K. Aghabayk, M. Sarvi, and W. Young, "A state-of-the-art review of car-following models with particular considerations

of heavy vehicles," *Transport Reviews*, vol. 35, no. 1, pp. 82–105, 2015.

[8] H. U. Ahmed, Y. Huang, and P. Lu, "A review of car-following models and modeling tools for human and autonomous-ready driving behaviors in micro-simulation," *Smart Cities*, vol. 4, no. 1, pp. 314–335, 2021.

[9] P. Gora, C. Katrakazas, A. Drabicki, F. Islam, and P. Ostaszewski, "Microscopic traffic simulation models for connected and automated vehicles (cavs)–state-of-the-art," *Procedia Computer Science*, vol. 170, pp. 474–481, 2020.

[10] H.-C. Jang and B.-Y. Li, "Vanet-enabled safety and comfort-oriented car-following system," in *Proceedings of the 2021 International Conference on Information and Communication Technology Convergence (ICTC)*, pp. 877–881, IEEE, Jeju Island, Korea, Republic of, October 2021.

[11] F. De Souza and R. Stern, "Calibrating microscopic car-following models for adaptive cruise control vehicles: multi-objective approach," *Journal of Transportation Engineering, Part A: Systems*, vol. 147, no. 1, 2021.

[12] W. Guo, Y. Li, Y. Li, J. Tan, and Z. Guo, "Research on multi-mode autonomous car-following model based on driving simulator," in *Proceedings of the 2019 34rd Youth Academic Annual Conference of Chinese Association of Automation (YAC)*, pp. 631–636, IEEE, Jinzhou, China, June 2019.

[13] A. B. Ims and H. B. Pedersen, "Simulation of automated vehicles in aimsun," https://9pdf.net/documd-of-automated-vehicles-in-aimsun.htmlMaster's thesis, NTNU, Norway, 2021, https://9pdf.net/documd-of-automated-vehicles-in-aimsun.htmlMaster's thesis.

[14] N. J. Goodall and C.-L. Lan, "Car-following characteristics of adaptive cruise control from empirical data," *Journal of Transportation Engineering, Part A: Systems*, vol. 146, no. 9, Article ID 04020097, 2020.

[15] M. Saidallah, A. El Fergougui, and A. E. Elalaoui, "A comparative study of urban road traffic simulators," in *MATEC Web of Conferences,* vol. 81, EDP Sciences, Article ID 05002, 2016.

[16] P. Sukennik, "Deliverable 2.5 Micro-simulation Guide for Automated Vehicles," 2018, https://www.h2020-coexist.eu/wp-content/uploads/2018/11/D2.5-Micro-simulation-guide-for-automated-vehicles.pdf.

[17] P. T. V. Vissim, "PTV vissim 10 user manual. PTV Planung Transport Verkehr AG," 2018, https://usermanual.wiki/Document/Vissim20102020Manual.1098038624.pdf.

[18] M. Zhu, X. Wang, A. Tarko, and S. Fang, "Modeling car-following behavior on urban expressways in shanghai: a naturalistic driving study," *Transportation Research Part C: Emerging Technologies*, vol. 93, pp. 425–445, 2018.

[19] L. Elefteriadou, *An introduction to traffic flow theory*, Vol. 84, Springer, Berlin, Germany, 2014.

[20] B. Higgs, M. Abbas, and A. Medina, "Analysis of the wiedemann car following model over different speeds using naturalistic data," in *Procedia of RSS Conference*, pp. 1–22, 2011, https://onlinepubs.trb.org/onlinepubs/conferences/2011/RSS/3/Higgs,B.pdf.

[21] U. Durrani, C. Lee, and H. Maoh, "Calibrating the wiedemann's vehicle-following model using mixed vehicle-pair interactions," *Transportation Research Part C: Emerging Technologies*, vol. 67, pp. 227–242, 2016.

[22] U. Durrani and C. Lee, "Calibration and validation of psychophysical car-following model using driver's action points and perception thresholds," *Journal of Transportation Engineering, Part A: Systems*, vol. 145, no. 9, Article ID 04019039, 2019.

[23] J. Bierstedt, A. Gooze, C. Gray, J. Peterman, L. Raykin, and J. Walters, "Effects of next-generation vehicles on travel demand and highway capacity," *FP Think Working Group*, vol. 8, pp. 10-11, 2014, https://issuu.com/fehrandpeers/docs/fp_think_next_gen_vehicle_white_paper_final.

[24] W. Atkins, "Research on the Impacts of Connected and Autonomous Vehicles (Cavs) on Traffic Flow," 2016, https://www.gov.uk/government/publications/driverless-vehicles-impacts-on-traffic-flow.

[25] V. Zeidler, H. S. Buck, L. Kautzsch, P. Vortisch, and C. M. Weyland, "Simulation of autonomous vehicles based on wiedemann's car following model in ptv vissim," in *Proceedings of the 2019 98th Annual Meeting of the Transportation Research Board (TRB)*, pp. 13–17, Washington, DC, USA, January 2019.

[26] V. Rossen, "Autonomous and cooperative vehicles and highway capacity: a theoretical model approach for vehicle automation and communication on Dutch highway road segments, focused on non-platoon based care-following behavior," http://essay.utwente.nl/76615/Master thesis, University of Twente, Netherlands, 2018, http://essay.utwente.nl/76615/Master thesis.

[27] P. Sukennik, V. Zeidler, and J. van Etten, "Deliverable 2.6 Technical report on data collection and validation," 2018, https://www.h2020-coexist.eu/wp-content/uploads/2018/10/D2.6-Technical-report-on-data-collection-and-validation-process_FINAL.pdf.

[28] E. Aria, J. Olstam, and C. Schwietering, "Investigation of automated vehicle effects on driver's behavior and traffic performance," *Transportation Research Procedia*, vol. 15, pp. 761–770, 2016.

[29] J. Piao and M. McDonald, "Advanced driver assistance systems from autonomous to cooperative approach," *Transport Reviews*, vol. 28, no. 5, pp. 659–684, 2008.

[30] ISO, "Intelligent Transport Systems - Adaptive Cruise Control Systems - Performance Requirements and Test Procedures," 2018, https://www.h2020-coexist.eu/wp-content/uploads/2018/10/D2.6-Technical-report-on-data-collection-and-validation-process_FINAL.pdf.

[31] V. Milanés and S. E. Shladover, "Modeling cooperative and autonomous adaptive cruise control dynamic responses using experimental data," *Transportation Research Part C: Emerging Technologies*, vol. 48, pp. 285–300, 2014.

[32] R. Prabha and M. G. Kabadi, "Overview of data collection methods for intelligent transportation systems," *International Journal of Engineering Science*, vol. 5, no. 3, pp. 16–20, 2016.

[33] J. Balsa-Barreiro, P. M. Valero-Mora, M. Menéndez, and R. Mehmood, "Extraction of naturalistic driving patterns with geographic information systems," *Mobile Networks and Applications*, pp. 1–17, 2020.

[34] O. Carsten, K. Kircher, and S. Jamson, "Vehicle-based studies of driving in the real world: the hard truth?" *Accident Analysis & Prevention*, vol. 58, pp. 162–174, 2013.

[35] H. Zhou, K. Kamijo, M. Itoh, and S. Kitazaki, "Effects of explanation-based knowledge regarding system functions and driver's roles on driver takeover during conditionally automated driving: a test track study," *Transportation Research Part F: Traffic Psychology and Behaviour*, vol. 77, pp. 1–9, 2021.

[36] P. A. Anand, P. Atmakuri, V. S. R. Anne et al., "Calibration of vehicle-following model parameters using mixed traffic trajectory data," *Transportation in Developing Economies*, vol. 5, no. 2, pp. 18–11, 2019.

[37] C. Buisson, W. Daamen, V. Punzo, P. Wagner, M. Montanino, and B. Ciuffo, "Calibration and validation principles," *Traffic*

Simulation and Data: Validation Methods and Applications, pp. 89–118, 2014.

[38] V. Punzo and F. Simonelli, “Analysis and comparison of microscopic traffic flow models with real traffic microscopic data,” *Transportation Research Record*, vol. 1934, no. 1, pp. 53–63, 2005.

[39] E. Brockfeld, R. D. Kühne, and P. Wagner, “Calibration and validation of microscopic traffic flow models,” *Transportation Research Record*, vol. 1876, no. 1, pp. 62–70, 2004.

[40] A. Sharma, Z. Zheng, and A. Bhaskar, “Is more always better? the impact of vehicular trajectory completeness on car-following model calibration and validation,” *Transportation Research Part B: Methodological*, vol. 120, pp. 49–75, 2019.

[41] V. Punzo, M. Montanino, and B. Ciuffo, “Do we really need to calibrate all the parameters? variance-based sensitivity analysis to simplify microscopic traffic flow models,” *IEEE Transactions on Intelligent Transportation Systems*, vol. 16, no. 1, pp. 184–193, 2015.

[42] I. Soria, L. Elefteriadou, and A. Kondyli, “Assessment of car-following models by driver type and under different traffic, weather conditions using data from an instrumented vehicle,” *Simulation Modelling Practice and Theory*, vol. 40, pp. 208–220, 2014.

[43] M. Treiber and A. Kesting, “Microscopic calibration and validation of car-following models–a systematic approach,” *Procedia-Social and Behavioral Sciences*, vol. 80, pp. 922–939, 2013.

[44] V. Punzo and M. Montanino, “Speed or spacing? cumulative variables, and convolution of model errors and time in traffic flow models validation and calibration,” *Transportation Research Part B: Methodological*, vol. 91, pp. 21–33, 2016.

[45] P. J. Jin, D. Yang, and B. Ran, “Reducing the error accumulation in car-following models calibrated with vehicle trajectory data,” *IEEE Transactions on Intelligent Transportation Systems*, vol. 15, no. 1, pp. 148–157, 2014.

[46] V. Punzo, B. Ciuffo, and M. Montanino, “Can results of car-following model calibration based on trajectory data be trusted?” *Transportation Research Record*, vol. 2315, no. 1, pp. 11–24, 2012.

[47] B. Ciuffo, V. Punzo, and M. Montanino, *The calibration of traffic simulation models. Report on the Assessment of Different Goodness of Fit Measures and Optimization Algorithms*, Publication Office of the European Union, Luxembourg, 2012.

[48] J. Gregory and C. Lin, *Constrained Optimization in the Calculus of Variations and Optimal Control Theory*, Chapman and Hall/CRC, Boca Raton, FL,USA, 2018.

[49] A. Kesting and M. Treiber, “Calibrating car-following models by using trajectory data: methodological study,” *Transportation Research Record*, vol. 2088, no. 1, pp. 148–156, 2008.

[50] L. Li, X. M. Chen, and L. Zhang, “A global optimization algorithm for trajectory data based car-following model calibration,” *Transportation Research Part C: Emerging Technologies*, vol. 68, pp. 311–332, 2016.

[51] M. Treiber and V. Kanagaraj, “Comparing numerical integration schemes for time-continuous car-following models,” *Physica A: Statistical Mechanics and Its Applications*, vol. 419, pp. 183–195, 2015.

[52] J. Kim and H. S. Mahmassani, “Correlated parameters in driving behavior models: car-following example and implications for traffic microsimulation,” *Transportation Research Record*, vol. 2249, no. 1, pp. 62–77, 2011.

[53] M. Zhu, X. Wang, and Y. Wang, “Human-like autonomous car-following model with deep reinforcement learning,” *Transportation Research Part C: Emerging Technologies*, vol. 97, pp. 348–368, 2018.

[54] M. Zhu, Y. Wang, Z. Pu, J. Hu, X. Wang, and R. Ke, “Safe, efficient, and comfortable velocity control based on reinforcement learning for autonomous driving,” *Transportation Research Part C: Emerging Technologies*, vol. 117, Article ID 102662, 2020.

[55] M. Saifuzzaman, Z. Zheng, M. Mazharul Haque, and S. Washington, “Revisiting the task–capability interface model for incorporating human factors into car-following models,” *Transportation Research Part B: Methodological*, vol. 82, pp. 1–19, 2015.

[56] J. H. Holland, *Adaptation in Natural and Artificial Systems: An Introductory Analysis with Applications to Biology, Control, and Artificial Intelligence*, MIT press, Cambridge, MA, USA, 1992.

[57] J. C. Spall, *Introduction to stochastic search and optimization: estimation, simulation, and control*, vol. 65, John Wiley & Sons, Hoboken, NJ, USA, 2005.

[58] R. M. James, B. E. Hammit, and S. D. Boyles, “Methods to obtain representative car-following model parameters from trajectory-level data for use in microsimulation,” *Transportation Research Record*, vol. 2673, no. 7, pp. 62–73, 2019.

[59] V. L. Knoop, M. Wang, I. Wilmink, D. M. Hoedemaeker, M. Maaskant, and E.-J. Van der Meer, “Platoon of sae level-2 automated vehicles on public roads: setup, traffic interactions, and stability,” *Transportation Research Record*, vol. 2673, no. 9, pp. 311–322, 2019.

[60] K. Othman, “Impact of autonomous vehicles on the physical infrastructure: changes and challenges,” *Design*, vol. 5, no. 3, p. 40, 2021.

[61] C. M. Weyland, M. V. Baumann, H. S. Buck, and P. Vortisch, “Parameters influencing lane flow distribution on multilane freeways in ptv vissim,” *Procedia Computer Science*, vol. 184, pp. 453–460, 2021.

[62] World Health Organization, “Global status report on road safety 2018,” https://www.who.int/pud789241565684Report, World Health Organization, Geneva, Switzerland, 2018, https://www.who.int/pud789241565684Report.

[63] J. Sangster, H. Rakha, and J. Du, “Application of naturalistic driving data to modeling of driver car-following behavior,” *Transportation Research Record*, vol. 2390, no. 1, pp. 20–33, 2013.

[64] G. Budan, K. Hayatleh, D. Morrey, P. Ball, and P. Shadbolt, “An analysis of vehicle-to-infrastructure communications for non-signalised intersection control under mixed driving behaviour,” *Analog Integrated Circuits and Signal Processing*, vol. 95, no. 3, pp. 415–422, 2018.